

Wetting transition and pretransitional thin films in binary liquids:  
alcohol/perfluoromethylcyclohexane mixtures studied by x-ray reflectivity

This article has been downloaded from IOPscience. Please scroll down to see the full text article.

2001 J. Phys.: Condens. Matter 13 5563

(<http://iopscience.iop.org/0953-8984/13/24/302>)

View [the table of contents for this issue](#), or go to the [journal homepage](#) for more

Download details:

IP Address: 171.66.16.226

The article was downloaded on 16/05/2010 at 13:31

Please note that [terms and conditions apply](#).

# Wetting transition and pretransitional thin films in binary liquids: alcohol/perfluoromethylcyclohexane mixtures studied by x-ray reflectivity

Anton Plech<sup>1</sup>, Uwe Klemradt and Johann Peisl

Sektion Physik, Ludwig-Maximilians-Universität München, Geschwister-Scholl-Platz 1, D-80539 München, Germany

Received 30 October 2000, in final form 4 May 2001

## Abstract

In this study the wetting transition at the liquid–vapour interface of binary organic liquid mixtures has been investigated by x-ray reflectivity. Mixtures of various isomeric alcohols with perfluoromethylcyclohexane (PFMC) served as model systems, with alcohol carbon numbers ranging from 1 to 4. Remarkably different pretransitional behaviour of the thin films below the wetting temperature was observed, which could be classified according to the carbon number. At two-phase coexistence, no pretransitional thin films could be detected for methanol and ethanol, whereas thin-to-thick-film transitions were found for propanol and butanol and their isomers. For 1-propanol and 2-propanol, the surface of the upper, alcohol-rich phase of the gravity-separated mixture displays a wetting transition at  $T_w = 31.5^\circ\text{C}$  and  $38.3^\circ\text{C}$ , respectively, where the thickness of a PFMC-rich film jumps from less than  $25\text{ \AA}$  to values exceeding the experimental resolution of about  $1200\text{ \AA}$ . For 1-butanol, 2-butanol and *i*-butanol, we found pretransitional film thicknesses increasing up to  $100\text{ \AA}$ , with wetting transitions at  $T_w = 45.0^\circ\text{C}$ ,  $34.2^\circ\text{C}$  and  $40.1^\circ\text{C}$ , respectively. In the single-phase region, the study of adsorption isotherms above  $T_w$  revealed novel behaviour of the adsorbed PFMC-rich film. We observed both a growing film thickness and a significantly changing composition as the coexistence line was approached. Nevertheless, the variation of the excess adsorption with distance from coexistence could still be described by a power law.

## 1. Introduction

Binary liquid mixtures represent valuable model systems for the study of wetting behaviour and phase transitions at the liquid–vapour interface. The phase diagrams of a large variety of systems are experimentally well accessible, and liquids offer also the advantage that defects and other difficulties known from the preparation of solid surfaces are largely absent. Extensive

<sup>1</sup> Author to whom any correspondence should be addressed. Present address: ESRF, BP 220, F-38043 Grenoble Cédex, France.

theoretical predictions have sketched a detailed picture of wetting transitions with respect to the order of the transition, its kinetics, the microscopic structure of the interfaces as well as their energetics [1]. Seminal experimental investigations have elucidated essential properties of wetting transitions, especially the first-order character of almost all wetting transitions in binary liquids studied so far, hysteresis and the nucleation of the surface phase [4] and wetting behaviour apart from two-phase coexistence, e.g. the prewetting transition line [5] (however, it should be noted that also an immiscible liquid system with a continuous wetting transition has been observed [3]). Open questions concern particularly the microscopic structure of the prewetting films and the appearance of precursor effects for the first-order wetting transition. Since more traditional methods in this field lack sensitivity on a molecular scale, we have addressed these questions by employing x-ray reflectivity at grazing angles, which is an excellent tool for the characterization of thin films and interfaces [6]. We chose binary mixtures of alcohols and perfluoromethylcyclohexane (PFMC,  $C_7F_{14}$ ) for our study since the density contrast of the components is sufficiently large for x-ray reflectivity experiments. The mixture with 2-propanol represents a classical system with a much lower surface tension of the gravity-separated lower PFMC-rich phase that promotes a non-universal discontinuous wetting transition at the upper phase–gas interface. For these systems, a discontinuous character of the wetting transitions was established very early, in addition to an interesting systematic variation of the wetting temperature  $T_w$  with the alcohol chain length [2, 18].

## 2. Experimental procedure

### 2.1. X-ray reflectivity

X-ray reflectivity at grazing angles can be described in terms of classical optics if the appropriate refractive index  $n$  is used in Fresnel's equations [7]. For x-rays,  $n$  is very close to one and is customarily written as  $n = 1 - \delta - i\beta$ . The dispersion and absorption corrections are given by

$$\delta = \frac{r_0}{2\pi} \lambda^2 \rho \quad (1)$$

$$\beta = \frac{\lambda\mu}{4\pi} \quad (2)$$

where  $r_0 = 2.818 \times 10^{-15}$  m denotes the classical electron radius,  $\lambda$  the x-ray wavelength,  $\rho$  the electron density of the material and  $\mu$  the linear absorption coefficient (for details see [7, 8]). With  $n$  less than unity, total external reflection occurs for x-rays incident from vacuum below a critical angle  $\alpha_c = \sqrt{2\delta}$  (typically a few tenths of a degree). As can be seen from equation (1), the critical angle is proportional to the x-ray wavelength and scales with the square root of the density. For  $\alpha \gg \alpha_c$  the ideal Fresnel reflectivity drops quickly with  $R_F \sim \delta\alpha^{-4}$ . Except for the vicinity of absorption edges, the reflectivity can be expressed as a function of just the modulus of the scattering vector:

$$Q = \frac{4\pi}{\lambda} \sin \alpha$$

which demonstrates formally the equivalence of energy-dispersive (ED) and angle-dispersive (AD) measurements if they are performed under experimental conditions where anomalous dispersion effects can be neglected. This is particularly the case for the present study, where organic materials with low- $Z$  components have been investigated using relatively hard x-rays.

The presence of thin films on a substrate as well as interfacial density gradients caused by roughness can be detected by reflectivity experiments with atomic-scale sensitivity. The structural information accessible with (specular) reflectivity measurements is the laterally

averaged electron-density profile along the surface normal (denoted here as the  $z$ -direction). This is expressed explicitly by equation (3), which demonstrates that the measured reflectivity  $R$ , if properly normalized to the ideal Fresnel reflectivity  $R_F$ , is related to the Fourier transform of the derivative of the actual density profile [9, 10]:

$$\frac{R}{R_F} = \left| \frac{1}{\rho_{Bulk}} \int \frac{d\langle\rho(z)\rangle}{dz} e^{iQz} dz \right|^2 \quad (3)$$

where  $\langle\rho(z)\rangle$  denotes the electron density averaged parallel to the surface. However, equation (3) is only valid within a kinematical approach. We used a generalized Parratt algorithm [11] for simulations, which takes into account properly multiple reflections, dispersion and absorption corrections by calculating the appropriate reflection coefficients at all interfaces and multiplying them within a matrix formalism. The experimental data were modelled by wetting layers of constant density, resulting in a piecewise-constant electron-density profile. To obtain a better description of the actual profile,  $\rho(z)$  was additionally smoothed by the inclusion of a (root mean square) interfacial roughness  $\sigma$  according to Névot and Croce [16], which replaces the finite-density jumps by a more realistic error function profile.

Interfaces of fluid phases are always corrugated by thermal fluctuations, the so-called capillary waves. These fluctuations have been shown to result in a broadening of the interfacial width  $\sigma$  [12]. The apparent (measured) width  $\sigma_{eff}$  is connected with the intrinsic interfacial width  $\sigma_{int}$ , temperature  $T$ , the interfacial tension  $\gamma$  and the experimental resolution by

$$\sigma_{eff}^2 = \sigma_{int}^2 + \frac{k_B T}{2\pi\gamma} \ln \left[ \frac{Q_{max}}{Q_{min}} \right] \quad (4)$$

where  $Q_{max}/Q_{min}$  is the ratio of two cut-off lengths. These correspond to the range of capillary wavelengths that actually contribute to  $\sigma_{eff}$  under the given experimental conditions. If the fluctuating liquid interface is located near to a rigid wall, a special behaviour is observed. In this case long-wavelength fluctuations are damped out as a function of the distance between the two interfaces, which leads to a sharper liquid interface and to a correlation of the corrugations of the two interfaces [13, 14].

## 2.2. Materials

We focused on mixtures of PFMC with alcohols of short and moderate chain lengths, including both isomers of propanol and three of the four isomers of butanol (see table 1). All liquids were used as received from the suppliers. The quoted purity was 99.8% for methanol and ethanol (Sigma-Aldrich). A value of 99.5% was quoted for the propanol liquids (Sigma-Aldrich) as well as for the butanol liquids (Fluka), with residual water or other isomers remaining below 0.05% each. Since PFMC is difficult to purify, it is usually available in technical-grade quality only (90–95%). The PFMC used here was 97% fully fluorinated (Alfa), the remainder essentially consisting of partly fluorinated molecules.

The miscibility phase diagram of several mixtures (systems 4 to 7) was determined by optical turbidity measurements to check the consistency with literature values, and also to improve the accuracy of experiments in the single-phase region close to the boundary. Figure 1 shows the results for two representative systems. The measured data points could be fitted with the same critical exponent for all systems and a mixture-dependent asymmetry parameter. The consolute temperatures derived from the fits are listed in table 1.

## 2.3. Experimental set-up and procedures

A major problem for scattering experiments at grazing angles is the preparation of a flat liquid surface, since the experimental resolution depends strongly on the radius of curvature

**Table 1.** Mixtures of alcohols  $C_nH_{2n+1}OH$  with  $C_7F_{14}$  investigated in this work. The accuracy of our temperature determinations is estimated to be  $0.2\text{ }^\circ\text{C}$  of relative error and  $0.4\text{ }^\circ\text{C}$  of absolute calibration error.

Alcohol	Carbon number $n$	Chemical formula	$T_c$ ( $^\circ\text{C}$ )	$T_w$ ( $^\circ\text{C}$ )	Reference
Methanol	1	$\text{CH}_3\text{-OH}$	157	82	[18]
Ethanol	2	$\text{CH}_3\text{-CH}_2\text{-OH}$	126	62	[18]
1-propanol	3	$\text{CH}_3\text{-CH}_2\text{-CH}_2\text{OH}$	131	22.7	[18]
				31.5	This work
2-propanol	3	$\text{CH}_3\text{-CHOH-CH}_3$	90.1	38.3	This work
			90.5	38.0	[2]
1-butanol	4	$\text{CH}_3\text{-(CH}_2)_2\text{-CH}_2\text{OH}$	131.5	45.0	This work
			131	7.5	[18]
2-butanol	4	$\text{CH}_3\text{-CH}_2\text{-CHOH-CH}_3$	99.5	34.2	This work
i-butanol	4	$(\text{CH}_3)_2\text{CH-CH}_2\text{OH}$	107.0	40.1	This work

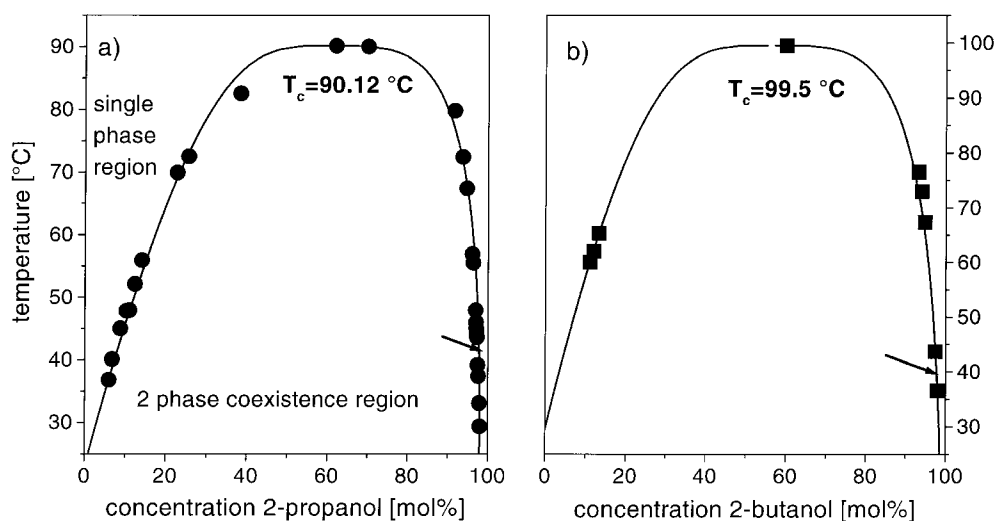


**Figure 1.** Miscibility phase diagrams of PFMC with (a) 2-propanol and (b) 2-butanol. The solid lines represent fits to experimentally determined coexistence points with a critical exponent  $\beta = 0.29$  [24]. The arrows indicate the region of interest investigated in this work.

encountered by the x-ray beam. The effective radius of curvature is not only determined by the geometry and material of the confining walls, but also by the depth of the liquid, since low-frequency surface waves can contribute significantly to a higher effective curvature. We found the best results by employing a specially designed vessel depicted in figure 2. It consists of a Teflon cylinder of 60 mm diameter with x-ray windows that were only thinned from the outside, so that a uniform contact line with only a slight upward meniscus developed at the entire boundary. As shallow liquids have been shown to attenuate effectively mechanically excited surface waves, the liquid in the centre of the cell was spread upon a glass wafer to form a film of about 0.6 mm thickness. In this way, we were able to obtain curvatures of more than 40 metres. A total liquid volume of about  $6\text{ cm}^3$  was used in the experiments, with

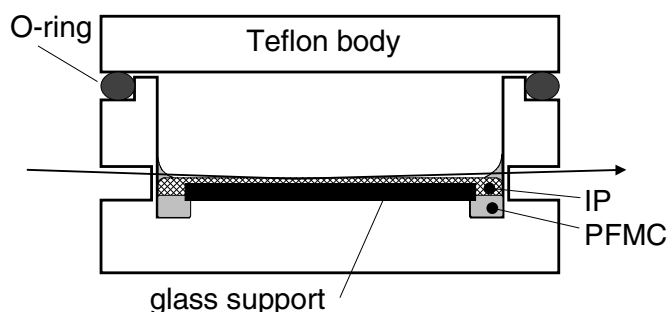


**Figure 2.** A cross-section of the experimental cell, sketched for a phase-separated liquid. The upper phase is spread over a glass wafer to maintain a shallow liquid.

most of the liquid being situated in a circular groove next to the wall. In the experiments involving phase separation, the glass support was solely covered by the upper phase, which, however, remained always in direct contact with the lower phase via the groove (cf. figure 2). The vessel was sealed with Viton rings and thermostatted by resistive heaters positioned in a highly symmetrically manner to minimize temperature gradients. The set-up was shielded from air convection etc by a nested arrangement of (x-ray-transparent) polymer foils. A LakeShore temperature controller (model 420) allowed us to achieve a long-term (24 h) thermal stability of better than 5 mK, which was the value measured at the *outer* surface of the vessel.

The entire cell was cleaned prior to the experiments with sulphuric acid; this was followed by a Millipore water rinse. All liquids were filled into the cell from the side through a sealable hole using syringes. Binary mixtures at two-phase coexistence were prepared by filling in PFMC first, followed by an appropriate amount of alcohol. This procedure was reversed for the preparation of mixtures located in the single-phase region, since only about 1 vol% PFMC needed to be added at the temperatures of interest (cf. figure 1). The preparation of a new mixture was always followed by a 24 h equilibration period. The equilibration time after changing temperature was at least 24 h for x-ray tube measurements and 12 h for synchrotron radiation experiments.

A significant part of the measurements were performed with a sealed-tube reflectometer designed for x-ray scattering from liquids [15, 17], which was operated in an angle-dispersive mode with Mo  $K\alpha$  radiation (17.46 keV) or in an energy-dispersive mode using the continuous spectrum up to 50 keV. Owing to the long equilibration times, extensive concentration series and temperature dependencies could only be studied with this instrument. However, its disadvantage is a relatively divergent beam that hinders the discrimination between diffuse scattering and specular reflectivity at high momentum transfer, thus inducing a large scatter of the data. Therefore, synchrotron radiation from HASYLAB (DESY) was used to cross-check the observations at selected points of the thermodynamic parameter space. This part of the measurements were carried out at the bending-magnet beamline D4, which is particularly suited for grazing-incidence experiments on liquids. The angle of incidence was varied by tilting the monochromator at a fixed Bragg angle with respect to the incident polychromatic beam, thus deflecting the monochromatic beam downwards onto the horizontal sample surface, which requires the automatic alignment of all beam elements along the trajectory of the incident and the exit beam. An x-ray energy of 14 keV was found a suitable compromise between resolution and momentum transfer on the surface. The specular and diffuse scattering was collected by a one-dimensional wire detector (Braun).

### 3. Results and discussion

#### 3.1. Two-phase coexistence

As an example for a thin-to-thick-wetting-film transition at two-phase coexistence, the reflectivity of a phase-separated 2-propanol/PFMC mixture is displayed in figure 3 together with fits according to Fresnel theory for two temperatures above and below the wetting temperature  $T_w$ . Below  $T_w$ , the reflectivity cannot be explained by a homogeneous 2-propanol-rich phase alone (which should not differ considerably from the reflectivity of pure 2-propanol), as indicated by the dashed line in figure 3. Instead, a very broad scaled thickness oscillation is discernible, which is the signature of a very thin, dense layer on top of the alcohol surface. This layer appears in equilibrium and is identified with the PFMC-rich prewetting film. Above  $T_w$  the structure of the reflectivity curve changes drastically with a new critical angle appearing. This is interpreted as indicating the presence of a wetting phase in the form of a very thick film, since no thickness oscillations are discernible. All wetting films exceed the instrumental resolution of about 1200 Å for synchrotron radiation experiments (600 Å for sealed-tube experiments).

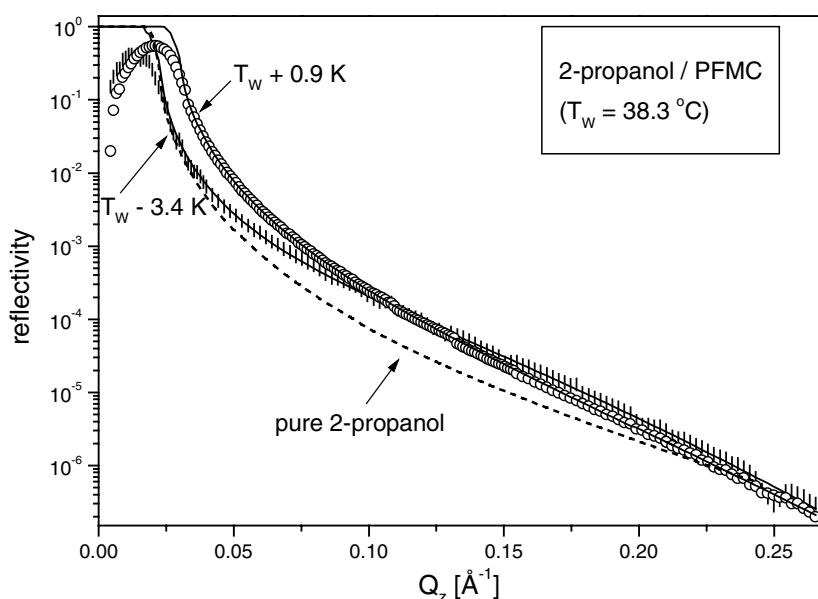


**Figure 3.** Specular reflectivities of the binary mixture 2-propanol/PFMC below and above the wetting transition temperature  $T_w$  (bars and circles, respectively). Fits to the experimental data are shown as full lines. A shift of the critical angle is clearly discernible. The simulation of the reflectivity of pure 2-propanol (broken line) indicates that below  $T_w$  a very thin layer is adsorbed on the 2-propanol surface.

It should be mentioned that the experimental data, despite illumination correction, do not exhibit the usual total-reflection regime. The reason for the discrepancy between simulation and experiment below the critical angle is depicted in figure 2: at extremely grazing angles, the reflected beam has to pass the meniscus, which affects the measured reflectivity by causing additional absorption. This angle-dependent effect causes intensity losses in the total-reflection regime that are difficult to correct for. It was therefore not possible to use the critical angle for data evaluation, e.g. to determine the density of the wetting phase. However, it was possible to circumvent this problem by normalizing the experimental data to absolute reflectivities, which

requires a careful measurement of the primary intensity. Since the density enters not only the critical angle but also the absolute reflectivity via  $\delta$  (cf. section 2.1), all relevant structural parameters could be derived from fits that exclude the total-reflection regime. The dynamic range of the reflectivity was invariably limited to seven orders of magnitude due to the diffuse scattering arising from capillary waves at the interfaces, and also to some extent due to diffuse bulk scattering arising from transmission through the meniscus.

Other alcohol/PFMC mixtures exhibit a qualitatively similar behaviour. Figure 4 shows data that indicate the temperature-dependent growth of the prewetting film in a 2-butanol/PFMC mixture. The measured reflectivities have been divided by the ideal Fresnel reflectivity of the alcohol. This procedure, inspired by e.g. formula (3), amplifies deviations from the theoretical reflectivity of a macroscopically thick (semi-infinite) phase, for example due to thickness oscillations from an adsorbed prewetting film. As can be seen from the frequency of the emerging undulations (see figure 4(a)), the thickness of the prewetting layer increases steadily with increasing temperature, until at a certain temperature suddenly no more oscillations are discernible and a new critical angle appears, which matches the density of a PFMC-rich wetting layer. This temperature was identified as the wetting temperature of the system.

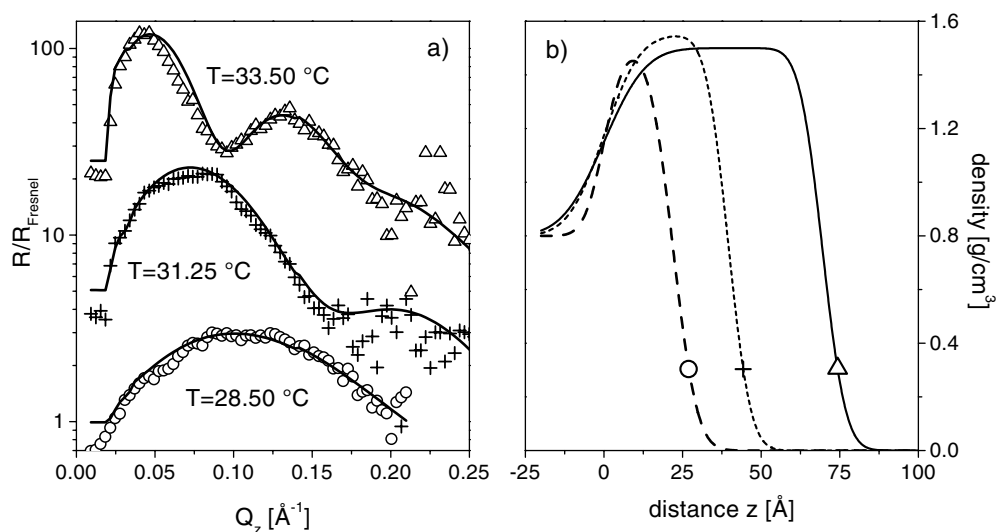


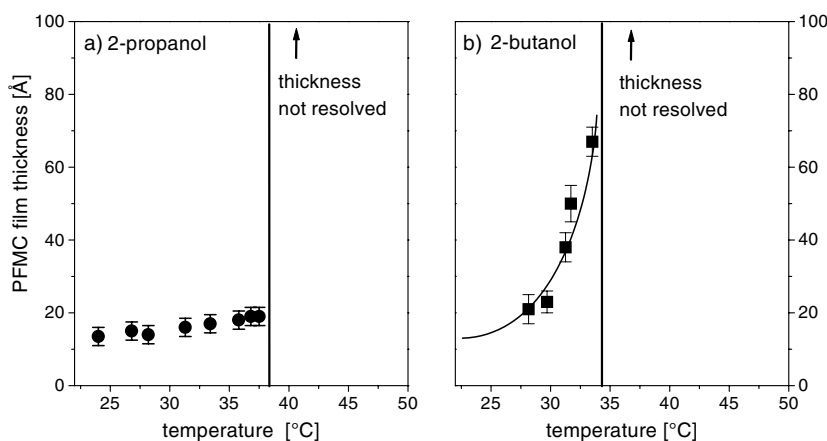
**Figure 4.** (a) Specular reflectivities of the binary mixture 2-butanol and PFMC for different temperatures below  $T_w$ . The experimental data have been divided by the ideal Fresnel reflectivity of the alcohol-rich phase (due to phase separation at  $T < T_c$ ). The curves are displaced by a factor of 5 for clarity; solid lines represent numerical fits to the data including interface roughness. (b) A sketch of the density profile perpendicular to the surface as derived from the fits.  $z = 0$  denotes the centre of the liquid–liquid interface.

Density profiles derived from fits to the reflectivity curves are shown in figure 4(b). All experimental data could be modelled by a single layer of the PFMC-rich phase adsorbed on the alcohol-rich phase. The density of the film is in agreement with the density of the PFMC-rich phase calculated from the experimentally determined phase diagram (figure 1). Mixing effects like excess volume were not accounted for in the calculation since the effect is smaller than our density resolution. The liquid–gas interface was characterized by an essentially constant root mean square roughness of about  $6 \pm 1\text{ } \text{\AA}$ . This result correlates with a computation of equation (4) for the given set-up, which yields  $6.8\text{ } \text{\AA}$  if the radii of the molecules are identified with  $\sigma_{\text{int}}$ . By contrast, the width of the liquid–liquid interface increased from  $6\text{ } \text{\AA}$  to  $11\text{ } \text{\AA}$  with



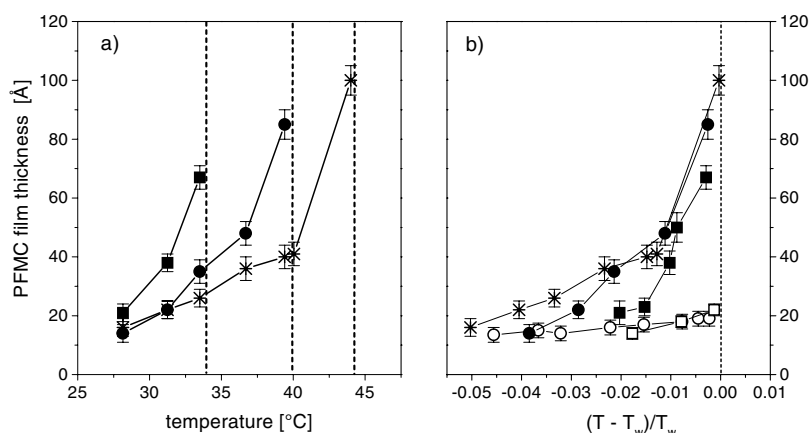
increasing film thickness (cf. figure 4(b)). This can be understood as a continuous decoupling of the interfacial capillary-wave fluctuations from the surface (see [6, 13]). Taking a value of  $Q_{max}/Q_{min} = 5 \times 10^4$  and an interfacial tension of  $13 \text{ mN m}^{-1}$  [18], the calculation is in agreement with the observed broadening of the liquid–liquid interface. There is no need to assume an increased intrinsic interface broadening  $\sigma_{int}$  above the natural molecular dimension, which is not surprising here, since the temperature is far below  $T_c$  and no critical divergence of a correlation length can be expected. Therefore it is justified to consider the surface enrichment as a sharp prewetting film which displays capillary-wave fluctuations, with fluctuations of the liquid–liquid interface being damped by the stiffer liquid–gas interface for thicknesses below  $40 \text{ \AA}$ .

Figure 5 summarizes the increase of the prewetting film thickness as a function of temperature for 2-propanol and 2-butanol mixtures. The vertical line denotes the wetting temperature determined as described above. For 2-propanol, within a temperature interval of less than  $0.05 \text{ K}$  a jump in thickness occurs from less than  $25 \text{ \AA}$  to macroscopic values (assessed to lie in the range of  $1500$  to  $2000 \text{ \AA}$ ). For 2-butanol, the jump in thickness is preceded by a much more pronounced (yet smooth) thickness increase towards the wetting transition, resulting in maximal prewetting film thicknesses of about  $100 \text{ \AA}$ . This type of behaviour is also observed if other alcohol isomers are investigated. Whereas discontinuous wetting transitions are found for all alcohols under investigation (see table 1), the growth behaviour of the pretransitional films falls into several distinct classes which depend strongly on the carbon number of the alcohol. For methanol and ethanol we did not find any indication for the existence of pretransitional wetting films. For 1-propanol and 2-propanol the thin films remain below  $25 \text{ \AA}$  even close to the transition. The  $C_4$ -alcohols are characterized by the growth of the pretransitional film up to  $100 \text{ \AA}$  as can be seen in figure 6(a). Figure 6(b) displays the behaviour of the pretransitional films as functions of the reduced temperature with respect to  $T_w$ , where the common behaviour is easiest to see.



**Figure 5.** The thickness of the thin PFMC-rich wetting film on the surface of the alcohol-rich phase as a function of temperature for (a) 2-propanol and (b) 2-butanol. The vertical lines denote the wetting transition temperature  $T_w$  as indicated by a jump in thickness of more than a decade, exceeding the experimental resolution.

Where a comparison is possible, table 1 indicates that our results for  $T_c$  agree well with previous work, whereas the data for  $T_w$  differ significantly (except for 2-propanol). The reason for these discrepancies is currently not clear. It could be argued that the purity of the PFMC



**Figure 6.** The thickness of the PFMC wetting film for different butanol and propanol isomers as functions of temperature (■: 2-butanol; ●: iso-butanol; \* : 1-butanol; ○: 2-propanol; □: 1-propanol). The vertical lines mark a strong increase in thickness beyond the experimental resolution. In (b) the values are plotted versus a reduced temperature based on  $T_w$ .

might play a role. Whereas this cannot be excluded with certainty, we find it highly unlikely that PFMC from the same batch should result in very unsystematic shifts of  $T_w$  ranging from 0 to 38 °C. It should also be mentioned that there is no indication that the liquids used in the previous work were significantly purer than those used here, since neither the purity of the PFMC nor the isomeric purity of the alcohols is addressed at all in reference [2, 18]. Instead reference [18] determines the wetting temperature by a macroscopic method, namely that of three phase contact angles. This is not directly comparable to molecularly resolved film thickness measurements, and it is possible that our reported pretransitional film growth can affect the apparent contact angle.

As for first-order characteristics of the wetting transitions observed here, we noticed that the wall of the sample cell acted as a nucleation centre. No hysteresis was observed, since wetting (as well as dewetting) occurred instantly (e.g., within the experimental time resolution) as the transition temperature was crossed<sup>2</sup>. By comparison, wetting phenomena of the same systems at a solid boundary involve time constants of hours owing to bulk diffusion [20].

It is an interesting question whether the observed discontinuous transitions precede a ‘hidden’ continuous transition. Such a behaviour is known from experiments with alkanes on water, where in general a continuous transition is found due to a change of sign of the effective Hamaker constant of the layered system. However, in the case of heptane this behaviour is perturbed by a discontinuity [5,21], which results in a smooth rise of the film thickness followed by a jump. While this behaviour appears to be very similar to the behaviour of the butanol mixtures, the physics is indeed different. We have calculated the Hamaker constant of the present systems from the optical index of refraction according to reference [22]. No indications for a hidden continuous transition preceded by a discontinuous transition were found, since the Hamaker constant does not change sign in the relevant temperature range (numerical values range between  $9.7 \times 10^{-21}$  J at room temperature and  $6.8 \times 10^{-21}$  J at 70 °C).

Therefore we conclude that the observed pretransitional film growth is intrinsically connected to the discontinuous wetting transitions, and is in particular related to the increasing

<sup>2</sup> A time resolution of ten minutes was achieved in the energy-dispersive mode, where the sample is illuminated by the x-ray ‘bremsspektrum’ and the reflected intensity is collected with an energy-dispersive detector [19]. This gives the reflectivity of a large  $Q$ -range without moving the sample.

alkane content of the rest of the alcohol molecules. Since only van der Waals interactions are described by the Hamaker constant, the above numerical values would imply complete wetting over the entire temperature range unless a destabilization of the wetting film occurs by an additional interaction, for example arising from short-range interactions (H bonds of the alcohols, structural forces) [19]. This competition of several interactions is found to be present in a surprisingly large quantity of known first-order transitions in binary liquids [3, 18, 23]. The discontinuous nature of the transition is then a result of the competing van der Waals and short-range interactions, which is the signature of a non-universal wetting transition.

### 3.2. Adsorption in the single-phase region

So far all experiments were located at the two-phase coexistence line, implying a phase-separated mixture in the sample container. It is well known that the discontinuity observed at the wetting transition extends into the single-phase region, giving rise to the so-called prewetting line. In the following we describe experiments in the single-phase region of the alcohol-rich side of the phase diagram (cf. figure 1). This region was further explored by keeping the sample at a constant temperature and increasing the concentration of PFMC successively towards two-phase coexistence. Of particular interest is the wetting film behaviour above  $T_w$ , where at coexistence a thick wetting film is present. From theory a continuous growth of the wetting film is expected, which is followed by a discontinuous increase as the prewetting line is crossed. Subsequently, the film thickness can diverge continuously as the coexistence is approached.

Measurements of the reflectivity at different concentrations of PFMC in a homogeneous alcohol-rich phase are displayed in figures 7 and 8 for 2-propanol and 2-butanol. The majority of the data have been taken at the sealed-tube reflectometer for reasons of time. As before,

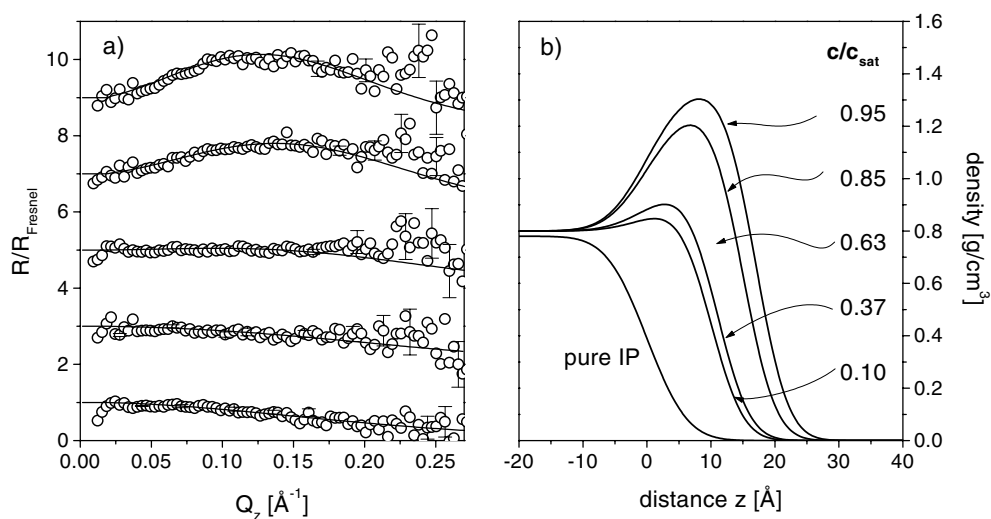


**Figure 7.** Normalized reflectivities of the 2-propanol/PFMC mixture in the single-phase region at 42.36 °C. The curves are displaced by 2 upwards with increasing 2-propanol concentration. Part (b) shows the corresponding density profiles as functions of concentration, given as fractions of the concentration  $c_{\text{sat}}$  at the coexistence line. Note that the density of pure PFMC is  $1.78 \text{ g cm}^{-3}$  and the density of the saturated PFMC-rich phase would be  $1.70 \text{ g cm}^{-3}$ .

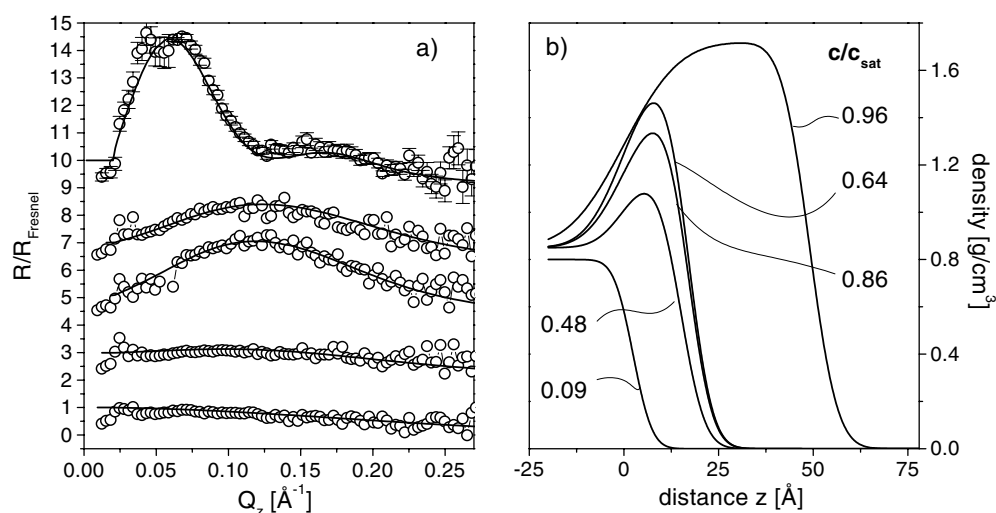


**Figure 8.** As figure 7, but for the 2-butanol/PFMC mixture at 39.05 °C. The uppermost curve is displaced relatively by 3. Note that the density of pure PFMC is 1.78 g cm<sup>-3</sup> and the density of the saturated PFMC-rich phase would be about 1.73 g cm<sup>-3</sup>.

the data have been scaled by the ideal Fresnel reflectivity of the alcohol in order to emphasize additional structure as a deviation from a horizontal line. On the right-hand side (figures 7(b) and 8(b)) density profiles resulting from the simulations are sketched. The reflectivity of 2-propanol shows a small increase relative to the Fresnel reflectivity, which can be interpreted as slight surface enrichment by PFMC. The reflectivity data were fitted with the same model as discussed in the previous section (single layers of a denser liquid on the alcohol surface). The interface roughnesses were kept constant as long as the curves displayed no detailed structure, with values derived from control experiments using synchrotron radiation. While the determination of the bulk density is subject to an error of 0.08 g cm<sup>-3</sup>, the relative density of the surface layer can be determined with a better resolution down to 0.03 g cm<sup>-3</sup>.

Whereas it is expected that the thickness of the film increases for concentrations which approach the concentration  $c_{sat}$  at coexistence, it is a surprising finding that also the density of the wetting film varies significantly with concentration. We find that the density reaches only just below the saturation concentration  $c_{sat}$  a value that corresponds to the density of the equilibrium binary mixture. The same holds for the mixture with 2-butanol, where the thickness growth is larger in agreement with the pretransitional growth at coexistence. When the concentration is further increased, the interface is readily wetted by the PFMC phase, and no thickness oscillations are discernible. In no case could a pretransitional film thickness be observed that exceeded the maximum pretransitional film thickness at coexistence. Therefore it can be concluded that we could not resolve the presumed prewetting line in our experiments, although it is obvious that the discontinuous nature of the transition is strongly imposed onto the single-phase region. These findings are in agreement with recent studies of various wetting phenomena, which show the tendency for there to be a prewetting line that is situated extremely closely to the coexistence line [3]. However, the new result here is that the increasing adsorption within the single-phase region is not only realized by an increasing film thickness, but also by a variable density of the adsorbed species at the surface. Only x-ray scattering methods have been able to investigate this problem so far, with the same behaviour being found for wetting phenomena of these mixtures at a solid boundary [20].

The thickness of the wetting film is not necessarily the relevant order parameter for wetting transitions of binary liquids, as already established by theoretical calculations [25]. Particularly for films with an inhomogeneous structure, the excess adsorption needs to be employed instead as a well-defined order parameter. This quantity has been determined for our data as the integral in the  $z$ -direction over the excess density (e.g., the density exceeding the density of the alcohol-rich phase). Figure 9 displays the calculated excess density at the surface in a double-logarithmic plot with respect to  $-\ln(c/c_{sat})$ . Under the approximation of an ideal mixture, the logarithm of  $c/c_{sat}$  is proportional  $\mu - \mu_c$ , where  $\mu_c$  denotes the chemical potential at coexistence. If algebraically decaying interactions govern the wetting behaviour, a power law is expected for the excess adsorption as a function of the chemical potential difference in the case of complete wetting. An exponent of  $1/3$  is predicted for non-retarded van der Waals interactions [26], whereas the inclusion of retardation effects results in even smaller exponents. The plot in figure 9 implies that a power law is still present, but an exponent of  $0.42 \pm 0.03$  is found for 2-propanol and  $0.58 \pm 0.15$  for 2-butanol. It should be noted that the power law is not expected to hold in the immediate vicinity of the wetting transition due to the non-universal, first-order nature of the transition.

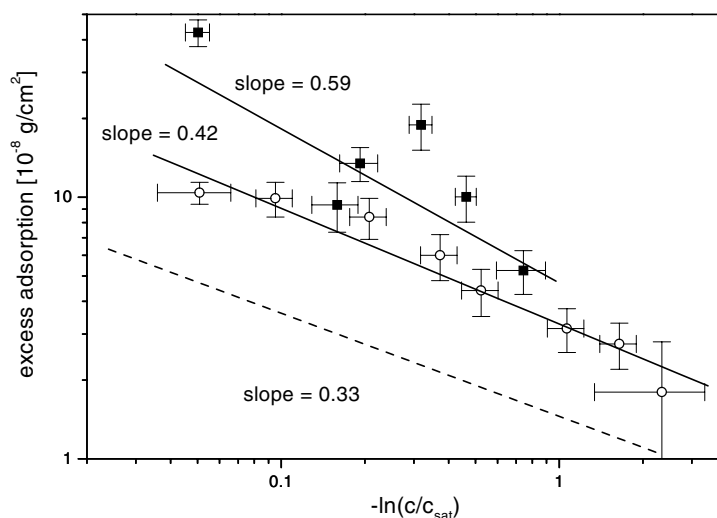


**Figure 9.** A chart of the excess adsorption (see the text) versus the logarithm of  $c/c_{sat}$  in a double-logarithmic plot. The solid lines represent straight-line fits to the data (■: 2-butanol; ○: 2-propanol). The theory of complete wetting yields an exponent of  $1/3$  (dashed line).

#### 4. Conclusions

The wetting behaviour of a series of binary mixtures of different alcohols with the per-fluorinated alkane PFMC has been explored by means of x-ray reflectivity. The method is capable of resolving the film thickness and density as well as additional interfacial properties like interfacial broadening. The common behaviour of all mixtures is the appearance of a discontinuous wetting transition at the surface of the alcohol-rich phase. Above the wetting temperature  $T_w$  a macroscopic film of the PFMC-rich phase is formed. From the temporal evolution of the system a nucleation of the transition from the contact line of the surface to the Teflon chamber can be concluded. Therefore the intrinsic nucleation behaviour was not

accessible. A striking new feature is found for pretransitional thin films of various mixtures. If the alcohols are grouped according to their carbon number, the results can be summarized as follows: the lowest alcohols did not show any thin films below  $T_w$ , whereas for propanol mixtures the thickness remained always below 25 Å. Much higher thicknesses up to 100 Å were observed for mixtures involving butanol isomers. Nevertheless, the jump in film thickness is also for these mixtures more than an order of magnitude. This behaviour raises the question of whether a further increase of the carbon number leads to even thicker pretransitional films resulting ultimately in a continuous transition. A natural end point is given by the pure alkanes, and indeed the continuous wetting of methylcyclohexane with PFMC [27] points to that possibility. No indications were found for a second hidden continuous transition related to a change of sign of the Hamaker constant. This observation leads to the question of the importance of classifying wetting transitions with regard to the strength of the discontinuity, which turned out to be relevant for displacive phase transitions in solids [28].

The interfacial structure of the wetting films was found to be in good agreement with capillary-wave theory. The liquid–gas interface displayed a constant width of 6.8 Å, whereas the width of the liquid–liquid interface increased up to 11 Å for thicker films. This is well understood by assuming a stiffer gas–liquid interface, from which the undulations of the liquid–liquid interface decouple with an increased spacing between the two interfaces. This behaviour can be studied in more detail if the diffuse scattering from capillary-wave fluctuations is systematically measured and compared to theory. This work is still in progress for the present systems.

Resolving the structure of the wetting films reveals unique features in experiments, where the mixture is situated in the single-phase region of the phase diagram. Upon changing the concentration towards coexistence, the chemical potential difference is changed similarly to that for gas–liquid wetting on a substrate. Here it is found that the thin adsorbed films forming in the single-phase region do not display the density that one would expect from the complementary phase. Instead, their density varies smoothly between the density of the majority phase (alcohol rich) and the minority phase (PFMC rich). Approaching two-phase coexistence, the growth of the wetting film is characterized by a density increase preceding the growth of the film up to equilibrium thicknesses as observed in the two-phase regime. In no experiment could a film thickness between the pretransitional state and the completely wet state be observed, which implies that a presumed prewetting line is situated rather close to the coexistence line, with  $c_{\text{prewetting}} > 0.97c_{\text{sat}}$ .

The novel behaviour of the wetting film growth correlates well with that found in other experiments, where 2-propanol/PFMC mixtures exhibit a wetting transition at a solid boundary [20]. There, a complementary situation occurs where an alcohol layer intrudes between the PFMC and a silicon surface. In the single-phase region wetting film structures were observed, which also showed a changing film density upon approaching coexistence, followed by a separate thickness growth regime. It seems quite possible that our findings point towards a more general behaviour of the wetting film growth process which consequently may also be found for other binary mixtures.

## Acknowledgments

Financial support by the Deutsche Forschungsgemeinschaft (Schwerpunkt ‘Benetzung und Strukturbildung an Grenzflächen’) is gratefully acknowledged. We wish to thank R Nowak and D Novikov for helpful advice at beamline D4. We appreciate fruitful discussions with F Schmid, W Fenzl, M Tolan and E Bertrand.

## References

- [1] Dietrich S 1988 Wetting phenomena *Phase Transitions and Critical Phenomena* vol 12, ed C Domb and J L Lebowitz (London: Academic) pp 1–218
- [2] Schmidt J W and Moldover M R 1983 *J. Chem. Phys.* **79** 379
- [3] Ragil K, Meunier J, Broseta D, Indekeu J and Bonn D 1996 *Phys. Rev. Lett.* **77** 1532
- [4] Bonn D, Bertrand E, Meunier J and Blossy R 2000 *Phys. Rev. Lett.* **84** 4661
- [5] Bonn D, Kellay H and Wegdam G H 1994 *J. Phys.: Condens. Matter* **6** A389
- [6] Tolan M 1999 *X-Ray Scattering from Soft-Matter Thin Films (Springer Tracts in Modern Physics vol 148)* (Heidelberg: Springer)
- [7] James R W 1962 *The Optical Principles of the Diffraction of X-rays* (Woodbridge, CT: Ox Bow)
- [8] Stanglmeier F, Lengeler B, Weber W, Göbel H and Schuster M 1992 *Acta Crystallogr. A* **48** 626
- [9] Pershan P S and Als-Nielsen J 1984 *Phys. Rev. Lett.* **52** 759
- [10] Als-Nielsen J, Jacquemain D, Kjaer K, Leveiller F, Lahav M and Leiserowitz L 1994 *Phys. Rep.* **246** 251
- [11] Parratt L G 1954 *Phys. Rev.* **95** 359
- [12] Braslau A, Pershan P S, Swislow G, Ocko B M and Als-Nielsen J 1988 *Phys. Rev. A* **38** 2457
- [13] de Gennes P-G 1985 *Rev. Mod. Phys.* **57** 827
- [14] Doerr A K, Tolan M, Prange W, Schlomka J-P, Seydel T, Press W, Smilgies D and Struth B 1999 *Phys. Rev. Lett.* **83** 3470
- [15] Metzger T H, Luidl C, Pietsch U and Vierl U 1994 *Nucl. Instrum. Methods A* **350** 398
- [16] Névoit L and Croce P 1980 *Rev. Phys. Appl.* **15** 761
- [17] Plech A, Klemradt U, Metzger H and Peisl J 1998 *J. Phys.: Condens. Matter* **10** 971
- [18] Schmidt J W 1987 *J. Colloid Interface Sci.* **122** 575
- [19] Plech A 2000 *Thesis Ludwig-Maximilians-Universität München* (Munich: Hieronimus)
- [20] Plech A, Huber M, Klemradt U and Peisl J 2000 *Europhys. Lett.* **49** 971
- [21] Shahidzadeh N, Bonn D, Ragil K, Broseta D and Meunier J 1998 *Phys. Rev. Lett.* **80** 3992
- [22] Israelachvili J 1992 *Intermolecular and Surface Forces* 2nd edn (London: Academic)
- [23] Ross D, Bonn D and Meunier J 1999 *Nature* **400** 737
- [24] Heady R B and Cahn J W 1973 *J. Chem. Phys.* **58** 896
- [25] Telo da Gama M M and Evans R 1983 *Mol. Phys.* **48** 229  
Telo da Gama M M and Evans R 1983 *Mol. Phys.* **48** 251
- [26] Pandit R, Schick M and Wortis M 1982 *Phys. Rev. B* **26** 5112
- [27] Kwon O D, Beaglehole D, Webb W W, Widom B, Schmidt J W, Cahn J W, Moldover M R and Stephenson B 1982 *Phys. Rev. Lett.* **48** 185
- [28] Clapp P C 1995 *J. Physique Coll.* **5** C8 11